Published OnlineFirst June 18, 2013; DOI: 10.1158/1078-0432.CCR-13-0522

Clinical Cancer Research

Predicting Drug Responsiveness in Human Cancers Using Genetically Engineered Mice

Jerry Usary, Wei Zhao, David Darr, et al.

Clin Cancer Res Published OnlineFirst June 18, 2013.

Published OnlineFirst June 18, 2013; DOI: 10.1158/1078-0432.CCR-13-0522

Clinical Cancer Research

Predicting Drug Responsiveness in Human Cancers Using Genetically Engineered Mice

Jerry Usary[1,2,3], Wei Zhao[1,2], David Darr[1], Patrick J. Roberts[1,2,4], Mei Liu[6], Lorraine Balletta[1,2], Olga Karginova[1,2], Jamie Jordan[1], Austin Combest[1,5], Arlene Bridges[1,5], Aleix Prat[7], Maggie C. U. Cheang[1,2,3], Jason I. Herschkowitz[8], Jeffrey M. Rosen[8], William Zamboni[1,5], Norman E. Sharpless[1,2,4], and Charles M. Perou[1,2,3]

Abstract

Purpose: To use genetically engineered mouse models (GEMM) and orthotopic syngeneic murine transplants (OST) to develop gene expression-based predictors of response to anticancer drugs in human tumors. These mouse models offer advantages including precise genetics and an intact microenvironment/immune system.

Experimental Design: We examined the efficacy of 4 chemotherapeutic or targeted anticancer drugs, alone and in combination, using mouse models representing 3 distinct breast cancer subtypes: Basal-like (*C3(1)-T-antigen* GEMM), Luminal B (*MMTV-Neu* GEMM), and Claudin-low (*T11/TP53*$^{-/-}$ OST). We expression-profiled tumors to develop signatures that corresponded to treatment and response, and then tested their predictive potential using human patient data.

Results: Although a single agent exhibited exceptional efficacy (i.e., lapatinib in the *Neu*-driven model), generally single-agent activity was modest, whereas some combination therapies were more active and life prolonging. Through analysis of RNA expression in this large set of chemotherapy-treated murine tumors, we identified a pair of gene expression signatures that predicted pathologic complete response to neoadjuvant anthracycline/taxane therapy in human patients with breast cancer.

Conclusions: These results show that murine-derived gene signatures can predict response even after accounting for common clinical variables and other predictive genomic signatures, suggesting that mice can be used to identify new biomarkers for human patients with cancer. *Clin Cancer Res; 1–11. ©2013 AACR.*

Introduction

Gene expression profiling has identified 5 molecular subtypes of breast cancer (Luminal A, Luminal B, Basal-like, HER2-Enriched, Claudin-low) and a Normal-like group, which show significant differences in epidemiologic associations and clinical features including survival (1–3). Mounting evidence suggests that these subtypes vary in their responsiveness to chemotherapeutics (2, 4–6) and to biologically targeted agents (7–9). Methods for selecting the optimal chemotherapeutic agent for each breast tumor subtype have yet to be determined. Instead, chemotherapy choices for patients with breast cancer have been mainly empiric and based upon large clinical trials using unselected patient populations, and population-based benefits. The basal-like subtype of breast tumor, of which the majority are also "triple-negative" breast cancers, is particularly challenging due to its lack of validated biologic targets [i.e., estrogen receptor (ER$^-$) and progesterone receptor (PR$^-$), and HER2 normal; refs. 10, 11]. Other breast cancer subtypes with poor prognosis also exist including the Luminal B subtype (2, 5) and the recently discovered Claudin-low subtype, which exhibits high numbers of tumor-initiating cells (12).

Genetically engineered mouse models (GEMM) have proven valuable for validating the causal role of oncogenes and tumor suppressor genes in cancer (13), but their use in efficacy testing is less mature, with most studies being low-throughput efforts examining model-specific compounds in small numbers of tumor-bearing mice (<50; ref. 14). Recently, academic and industry researchers have begun simultaneous efficacy testing at medium throughput, using larger numbers of compounds (5–50) in larger numbers of GEMMs (100–1000; refs. 15, 16). In particular, these efforts have attempted to mirror and inform ongoing human

Authors' Affiliations: [1]Lineberger Comprehensive Cancer Center, Departments of [2]Genetics and [3]Pathology and Laboratory Medicine, [4]Division of Hematology and Oncology, Department of Medicine, [5]School of Pharmacy, University of North Carolina at Chapel Hill, Chapel Hill, North Carolina; [6]Department of Gastroenterology, Tongji Hospital, Huazhong University of Science & Technology, Wuhan, China; [7]Translational Genomics Group, Vall d´Hebron Institute of Oncology (VHIO), Barcelona, Spain; and [8]Department of Molecular and Cellular Biology, Baylor College of Medicine, Houston, Texas

Note: Supplementary data for this article are available at Clinical Cancer Research Online (http://clincancerres.aacrjournals.org/).

Corresponding Author: Charles M. Perou, Lineberger Comprehensive Cancer Center, 450 West Drive, CB7295, University of North Carolina, Chapel Hill, NC 27599. Phone: 919-843-5740; Fax: 919-843-5718; E-mail: cperou@med.unc.edu

doi: 10.1158/1078-0432.CCR-13-0522

Published OnlineFirst June 18, 2013; DOI: 10.1158/1078-0432.CCR-13-0522

Translational Relevance

The identification of new predictive biomarkers is a difficult task, which often requires treatment of human patients with experimental drugs. Genetically engineered mouse models (GEMM) hold the promise of providing a preclinical arena for this early drug testing and possible biomarker discovery. A signature of chemotherapy response was identified through the use of credentialed GEMM of mammary cancer. This signature was then shown to predict neoadjuvant response in human patients with breast cancer. If validated in additional studies, this signature may show clinical value for selecting patients who will benefit from neoadjuvant anthracycline/taxane regimens, and shows the value of drug testing in mice as a means for identifying new biomarkers.

clinical trials, by testing novel therapeutics in faithful murine models as "coclinical trials" (17). Although this approach has been promising, we believe that an additional untapped power of medium-throughput GEMM testing is the ability to use murine models to identify biomarkers of response for human patients with cancer.

Previously, we conducted RNA expression profiling of 13 distinct GEMMs of breast cancer (12, 18) and compared these signatures with human expression subtypes using an across-species expression analysis. These analyses identified murine models that faithfully represent multiple human breast tumor subtypes including Basal-like tumors (*C3(1)-T-antigen*; ref. 19) and Luminal B tumors (*MMTV-Neu*; ref. 20). No single Claudin-low GEMM was identified, but an orthotopic, transplantable syngeneic tumor from a *BALB/c TP53*$^{-/-}$ mouse was found to exhibit a stable Claudin-low expression phenotype (12). In this work, we used these credentialed murine tumor models and determined their sensitivities to a variety of chemotherapeutic and biologically targeted agents in routine clinical use. This analysis identified a heterogeneity of responses to certain cytotoxics in the Basal-like model. We exploited this existence of sensitive and resistant tumors from GEMMs to develop genomic signatures of chemotherapy response, which we tested in a large, clinically annotated human cohort of patients with breast cancer.

Materials and Methods

Genetically engineered mouse models

All work was done under protocols approved by the University of North Carolina (UNC; Chapel Hill, NC) Institutional Animal Care and Use Committee. GEMMs of strain *FVB/n* carrying a transgene for *Tg(MMTVneu)202Mul/J* (*MMTV-Neu*; ref. 20) and *C3(1)SV40 T-antigen (C3(1)-T-antigen* or *C3-TAg*; ref. 21) were bred in-house and observed until the onset of a mammary tumor approximately 0.5 cm in any dimension. Tumors derived from *BALB/c TP53*$^{-/-}$ orthotropic mammary gland transplant line (T11) were passaged in *BALB/c* wild-type mice by subcutaneous injection of one half million cells resuspended in Matrigel into the flank as previously described (22). Mice were randomized into treatment groups and monitored with tumor growth measurements. Tumor volumes were measured by caliper in two dimensions and/or by ultrasound (Vevo 770 ultrasound imaging system; Visualsonics Inc.). Chemotherapy was started at time zero and repeated weekly for a total of 3 injections over a 21-day period. The mice were further assessed for long-term survival as follows: if after a 1-week break from treatment, a tumor increased in volume more than 1 mm in any dimension, then additional 3 cycles of therapy were initiated. This continued until either the mouse developed a tumor burden sufficient to warrant euthanasia (2 cm in any dimension or 3 tumors present) or until weight loss totaling 20% of the initial starting body mass was observed or because of any other severe health problems. Orally administered biologic inhibitors were given continuously with no dose interruption. In the case of a chemotherapeutic plus an oral inhibitor, the chemotherapy agent was dosed once weekly for 21 days and stopped until progression, whereas the small-molecule inhibitors were dosed continuously.

Compounds. Compounds were obtained from commercial sources: carboplatin (Hospira, Inc), cyclophosphamide (Hospira, Inc), doxorubicin (Bedford Laboratories), paclitaxel (Ivax Pharmaceuticals, Inc), erlotinib (Genentech, Inc), and lapatinib (GlaxoSmithKline). Oral biologic inhibitors (erlotinib and lapatinib) were milled into chow by Research Diets, Inc., whereas carboplatin and paclitaxel were delivered via intraperitoneal injection.

Treatments. The drug-specific approach to determine schedule and dose is described in Supplementary Table S5. A minimum tumor volume of approximately 0.5 cm in size was required for randomization into a treatment group (including a control group). Combination treatments were given at the same doses as the individual treatments. Chemotherapy was started at time zero and repeated weekly for over a 14-day (*T11/TP53*$^{-/-}$) or 21-day (*C3(1)-T-antigen* and *MMTV-Neu*) period.

Pharmacokinetic studies. Pharmacokinetic studies were conducted after administration of paclitaxel (Supplementary Fig. S1), erlotinib, and lapatinib (data not shown). For paclitaxel, 17 transgenic *FVB/n* mice bearing the *MMTV-Neu* transgene were administered a single intraperitoneal dose of paclitaxel at 10 mg/kg. Plasma and tumor samples (3 mice used at each time point; 2 mice used for the 48 hours time point) were collected at 0.083, 1, 4, 8, 24, and 48 hours after administration and flash frozen in liquid nitrogen. The samples were analyzed via liquid chromatography/tandem mass spectrometry as described previously (23). The concentration versus time profiles of paclitaxel in plasma and tumor are presented in Supplementary Fig. S1. The mean ± SD of paclitaxel C_{max} and area under the curve ($AUC_{0-\infty}$) in plasma following intraperitoneal administration were 2.1 μg/mL ± 1.5 and 6.3 μg/mL•hour, respectively. The mean ± SD of paclitaxel C_{max} and $AUC_{0-\infty}$ in tumor following intraperitoneal administration were 3.7 μg/g ± 2.1 and 42.4 μg/g•hour, respectively.

Published OnlineFirst June 18, 2013; DOI: 10.1158/1078-0432.CCR-13-0522

Response criteria. Tumor volume was calculated from two-dimensional measurements as Volume = $(\text{width})^2 \times (\text{length})/2$. The percent change in volume at 21 days was used to quantify response, except in the case of the *T11/TP53*$^{-/-}$ model where its faster growth rate required a 14-day treatment response assessment. Twenty-one day response was chosen as our primary response endpoint based on the fact that most of the untreated animals do not survive much longer than 21 days when starting with a tumor of more than 0.5 cm. Survival was measured from the first day of drug treatment.

Microarray analysis

DNA microarray analyses of murine tumors were conducted as described in Herschkowitz and colleagues (12). We used Agilent 4 × 44,000 feature mouse DNA microarrays and a common reference strategy. For hierarchical clustering analyses, the genes/rows were median centered, and clustering of arrays was conducted using Cluster v3.0 (24) with correlation centered genes and arrays, and centroid linkage. Array cluster viewing and display were conducted using JavaTreeview v1.1.4 (25).

Statistical analyses

Identification of significant differential genes in response to treatments. We conducted 2 unpaired two-class significance analysis of microarray (SAM; ref. 26) analyses to identify genes that showed differential expressions as following: (i) between carboplatin/paclitaxel-treated *C3(1)-T-antigen* tumors that responded versus those that did not and (ii) between carboplatin/paclitaxel-treated *C3(1)-T-antigen* tumors versus those untreated. The primary SAM analysis to identify tumor response-related genes included 3 responding tumors (shrinkage >20%) versus 9 nonresponding tumors (growth >20%). The secondary SAM analysis to identify treatment of upregulated or downregulated genes included 7 untreated tumors versus the 12 treated tumors. Two gene lists were obtained with a false discovery rate (FDR) of 1%: 348 genes (428 probes) showing significantly high expression in the untreated samples (called UNTREATED) and 61 genes (74 probes) showing significantly high expression in the samples from responders (called RESP-HIGH); the identified genes are listed in Supplementary Table S2. Using the Mouse Genome Database (27), these lists were converted to orthologous human genes. To refine the list of these candidate genes relevant to human tumors, a hierarchical clustering analysis of these orthologous human gene lists was conducted using the 337 tumor samples from Prat and colleagues (1). From these clusters, we chose a dendrogram node based on the criteria that it would include the largest number of highly expressed genes and have a node correlation of more than 0.4. Supplementary Figure S2B illustrates the gene set called UNTREATED-HUM that includes 30 unique genes. Supplementary Figure S2D illustrates the gene set called RESP-HUM that includes 12 unique genes.

In the UNC337 human tumors sets, these 2 gene lists showed "homogeneous" expression patterns, and thus we decided that taking the mean of the genes within each list/dendrogram node was the most appropriate method to assign the signature score for each tumor sample. In brief, an UNTREATED-HUM score was assigned to each test sample by taking the mean of the 26 genes in the list. A RESP-HUM score was assigned to each test sample by taking the mean of the 12 genes in the list. Because we also aimed to compare the performance of these 2 signatures as well as including published genomic signatures, we standardized the signature scores with a standard deviation equivalent to 1 to bring all the signature scores to the same scale. We applied this same methodology to 2 independent datasets of neoadjuvant human tumors described below.

Association of the identified signatures with tumor response for neoadjuvant anthracycline/taxane containing chemotherapy regimens. The performance of UNTREATED-HUM and RESP-HUM signatures to predict pathologic complete response (pCR) was first tested on 462 patients with HER2 normal tumors in MD Anderson Cancer Center (Houston, TX) dataset (Hatzis and colleagues; ref. 28; Gene Expression Omnibus; GEO # GSE25066) and validated on 81 patients with HER2 normal tumors in the Osaka University Hospital dataset (Miyake and colleagues; ref. 29; GEO # GSE32646). Patients on both datasets were treated with neoadjuvant anthracycline/taxane containing regimens. Univariable logistic regression analysis was used to assess the OR and significance of the 2 signatures to predict pCR. Multivariable logistic regression analysis was used to determine the adjusted OR and significance taking into account for the standard clinical variables measured at baseline and other published genomic signatures as appropriate. The AUC value was calculated from the Receiver Operating Characteristics analysis of the univariable and multivariable logistic model, respectively. The published genomic signatures included the PAM50 intrinsic subtypes (2), Claudin-low predictor (1), and 11-gene proliferation signature (9); we also included signatures developed by Hatzis and colleagues [including Hatzis sensitivity to endocrine therapy (SET) index, Hatzis signature chemosensitive RCB-I predict, and Hatzis signature chemoresistance (RCB-III predict)] that were available for the dataset (28). Finally, survival outcome data after neoadjuvant treatment were available for the Hatzis and colleagues dataset, and Kaplan–Meier analysis and log-rank test were used to determine the differential survival estimates of the 2 signatures to distant relapse-free survival (DRFS; ref. 28).

Results

Sensitivity of GEMMs to chemotherapeutic agents

Our ultimate goal was to use GEMMs to develop predictors of therapeutic response for humans. Details of the workflow are outlined in the study design (Fig. 1). As a first step, we tested 3 different mammary cancer GEMMs with multiple therapeutics to find a GEMM and a drug regimen, which gave a range of responses; from this GEMM, we then profiled sensitive and resistant tumors to identify a signature associated with response. We first therefore, determined the sensitivity of 3 distinct GEMMs/OSTs models of human breast cancer subtypes versus 2 cytotoxic chemotherapeutics

Published OnlineFirst June 18, 2013; DOI: 10.1158/1078-0432.CCR-13-0522

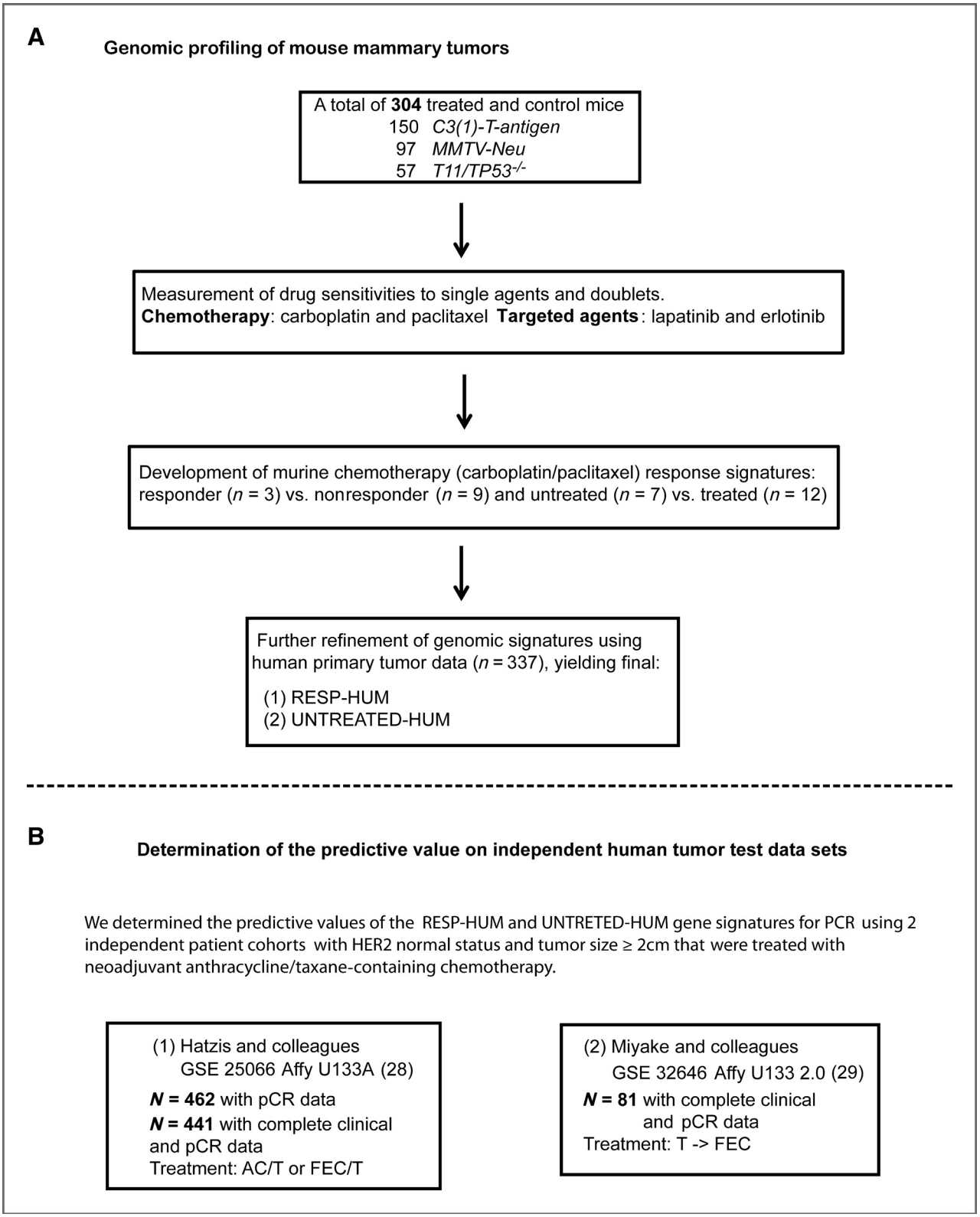

Figure 1. Study design overview. A, drug treatment and genomic profiling of mouse mammary tumors for the development of chemotherapy response signatures. B, testing of genomic signatures on 2 human tumor neoadjuvant treatment data test datasets.

Published OnlineFirst June 18, 2013; DOI: 10.1158/1078-0432.CCR-13-0522

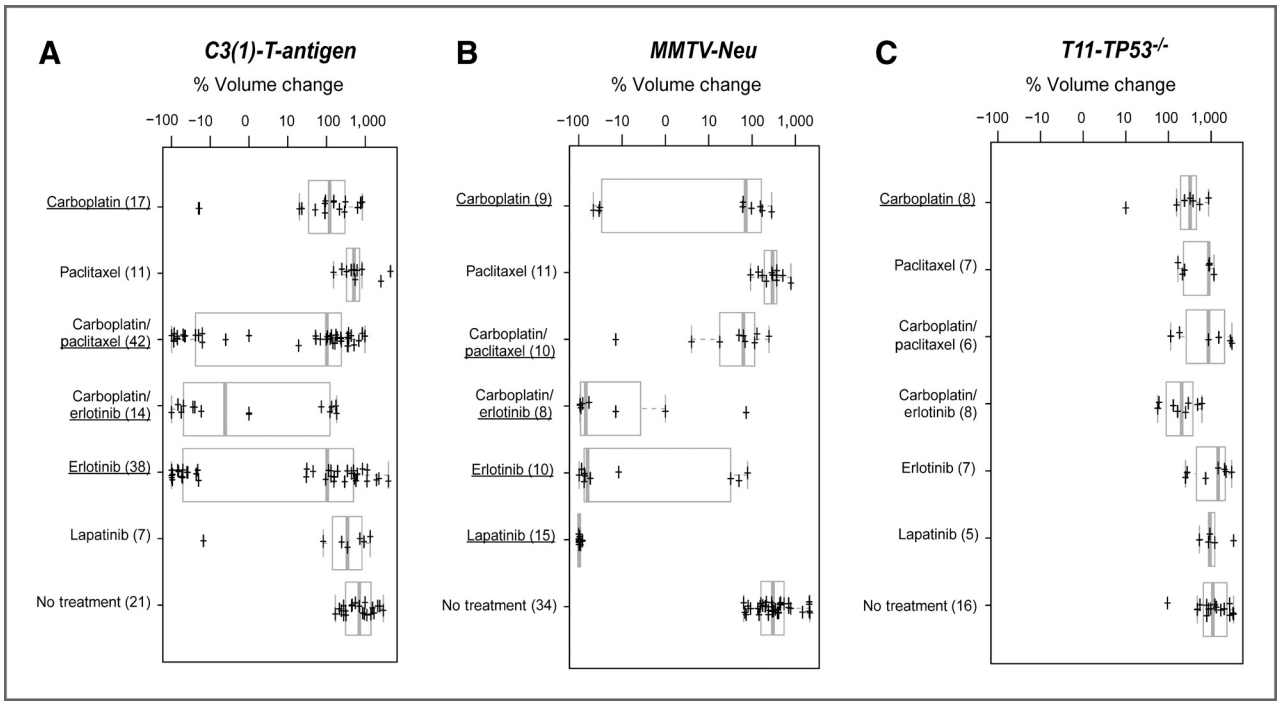

Figure 2. Short-term treatment responses for 3 mouse models of mammary cancer. Box and whisker plots are shown as measures of tumor responsiveness. In each case, 2 to 3 cycles of therapy was administered for all chemotherapeutics (1 dose/week), whereas in the case of erlotinib and lapatinib, the drug was continuously administered via the chow. Tumor size was measured at baseline and at weekly intervals thereafter. The change in tumor volume over a 21-day treatment period is plotted for *C3(1)-T-antigen* model (A), *MMTV-Neu* model (B), and *T11/TP53*$^{-/-}$ (C) model; note that the *T11/TP53*$^{-/-}$ model is based upon a 14-day treatment period due to its faster growth rate. Drugs that elicited a statistically significant response as assessed by a *t* test when compared with its matched untreated controls are identified by being underlined. The number of animals in each treatment group is indicated in parentheses.

and 2 small-molecule kinase inhibitors. The models used were *C3(1)-T-antigen*, *MMTV-Neu*, and *T11/TP53*$^{-/-}$, with these models chosen based on their similarity in gene expression to Basal-like, Luminal B, and Claudin-low human tumor subtypes, respectively (12, 18). Tumor volume changes at 21 days (or 14 days in the *T11/TP53*$^{-/-}$ model), and long-term survival were the primary endpoints. Response at 21 days (or 14 days for *T11/TP53*$^{-/-}$) was measured for 304 treated and control mice (150 *C3(1)-T-antigen*, 97 *MMTV-Neu*, 57 *T11/TP53*$^{-/-}$) with the percent volume change of each model's nontreated controls (i.e., growth rate) shown in Fig. 2 (bottom rows). Although there was overlap in the average growth rates of tumors from each GEMM, the untreated *T11/TP53*$^{-/-}$ tumors grew significantly faster than their *MMTV-Neu* counterparts ($P < 0.01$, Student *t* test), with the *C3(1)-T-antigen* model exhibiting an intermediate growth rate (Fig. 2).

With the growth kinetics of these models established, we next tested 2 chemotherapeutics that are widely used to treat many solid epithelial human cancers, namely paclitaxel and carboplatin. Although the standard of care for most patients with breast cancer is doxorubicin/cyclophosphamide with or without a taxane (i.e., AC-T; ref. 30), platinum agents (carboplatin/cisplatin) are also gaining in use (31), and thus are relevant to breast cancers, especially triple-negative breast cancers (TNBC). As a single agent, carboplatin elicited a modest but significant responses in all 3 models, whereas paclitaxel alone elicited no response; however, systemic and tumor drug delivery was confirmed for paclitaxel (Supplementary Fig. S1).

Next we tested the commonly used chemotherapy doublet of carboplatin/paclitaxel (CT). A varied response profile was seen for the CT combination where the combination showed no activity in the *T11/TP53*$^{-/-}$ model, and only modest activity in the *MMTV-Neu* model. Importantly, in the *C3(1)-T-antigen* model, a clear bimodal response was observed to the CT combination: approximately 2 of the 3 tumors showed little response and approximately 1 of the 3 showed near complete regression (Fig. 2A). This finding is in accord with the observation that human Basal-like tumors exhibit an approximately 30% to 40% pCR rate to taxane-containing neoadjuvant regimens, whereas the other 60% to 70% show residual disease and a worse overall survival (1, 5, 10).

Sensitivity to targeted agents

Two classes of biologically targeted agents are used in patients with breast cancer: agents blocking ER/PR signaling (e.g., tamoxifen or aromatase inhibitors) and drugs targeting HER2 (e.g., trastuzumab and lapatinib). Given that none of our GEMMs were ER$^+$ or PR$^+$ (12), we chose to focus on the HER2/EGFR family of kinases by using the small-molecule inhibitor lapatinib (which targets HER2/ERBB2 primarily; ref. 27), and the EGF receptor (EGFR) inhibitor erlotinib (32). In the *MMTV-Neu* model, erlotinib and lapatinib were

Published OnlineFirst June 18, 2013; DOI: 10.1158/1078-0432.CCR-13-0522

both highly effective, with lapatinib causing nearly 100% regression in all *MMTV-Neu* tumors. Conversely, neither erlotinib nor lapatinib was effective at reducing the growth rate of the *T11/TP53*$^{-/-}$ tumors. Lapatinib was similarly ineffective in the *C3(1)-T-antigen* tumors, but as was the case for the CT doublet, erlotinib showed potent activity in a subset (~40%) of treated mice. These data show that HER2/EGFR inhibitors exhibit potent activity in the *Neu/ERBB2/HER2*-driven model as expected, and provide further evidence for at least 2 subtypes of *C3(1)-T-antigen* tumors with regard to therapeutic sensitivity.

We also assessed the effects of anticancer therapies on the overall survival of tumor-bearing mice. Baseline survival for the *MMTV-Neu* (29 days) and *C3(1)-T-antigen* models (33 days) was similar in the absence of therapy, whereas the *T11/TP53*$^{-/-}$ animals showed significantly shorter median survival (15 days; Fig. 3). In the *MMTV-Neu* model, single-agent lapatinib (and to some extent erlotinib) greatly extended lifespan from a median of 29 to 154 days (Fig. 3B). Conversely, no single or combination regimen was able to extend survival in the *C3(1)-T-antigen* or *T11/TP53*$^{-/-}$ models.

Development of murine chemotherapy response signatures

A heterogeneous response to CT was seen in the *C3(1)-T-antigen* tumors that ranged from progressive disease to complete response (Fig. 2A). We sought to explore these findings and develop a genomic predictor of this response using this GEMM by conducting RNA expression profiling of treated versus untreated tumors. For these experiments, we treated *C3(1)-T-antigen* tumors with carboplatin/paclitaxel for 2 or 3 cycles and measured response ($n = 12$), and

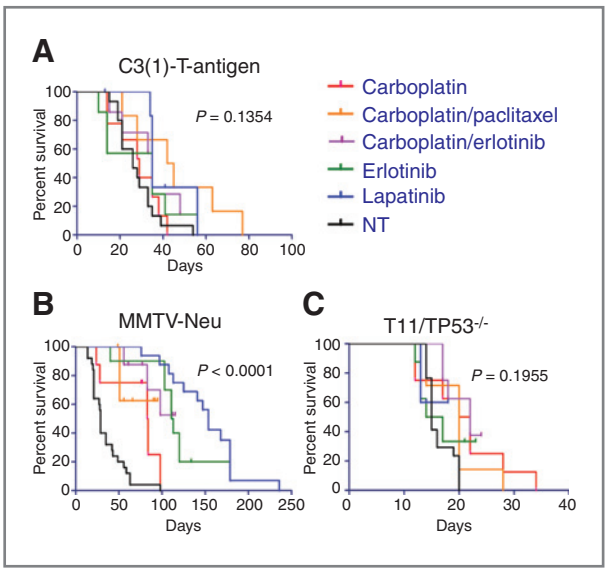

Figure 3. Long-term survival results for 3 mouse models of mammary cancer. Kaplan–Meier analyses for overall survival of tumor-bearing mice were conducted. *C3(1)-T-antigen* (A), *MMTV-Neu* (B), and *T11/TP53*$^{-/-}$ (C) results for chemotherapeutic treatments, targeted agents, and combinations. A log-rank test was conducted to determine significance of all treatment groups and is shown. NT, not treated.

then harvested the tumor for molecular analysis. In addition, an independent set of 7 untreated tumors was used as the nontreated controls (Supplementary Table S1).

SAM (26) was used to derive 2 sets of differentially expressed genes by (A) comparing those mice that responded to treatment ($n = 3$) with those that did not ($n = 9$), and by (B) comparing the untreated ($n = 7$) with treated tumors ($n = 12$; Supplementary Tables S1 and S2). When testing untreated versus treated tumors at a FDR of 1%, this analysis identified 428 probes corresponding to 348 mouse genes that were more highly expressed in untreated tumors (called UNTREATED gene list; Supplementary Table S2A); a Gene Ontology (GO) analysis of the UNTREATED list identified multiple significant terms including "cellular macromolecule metabolic process," "nucleic acid metabolic process," "regulation of macromolecule biosynthetic process," "chromosome organization," "DNA metabolic process," and "cell cycle." We applied a modules/signatures analysis to the untreated versus treated tumors where we examined whether 302 previously defined expression signatures (33) varied with treatment (Supplementary Table S3). This modules/signatures analysis showed that multiple signatures of fibroblasts/extracellular matrix, and signatures of the Claudin-low phenotype (1, 18) were more highly expressed after treatment, with this last result recapitulating findings observed in postchemotherapy-treated human tumors (34). Multiple signatures decreased after treatment including one of proliferation and one of HER1–RAS pathway activation. These data show that CT treatment induced expression of genes associated with Claudin-low/mesenchymal phenotype, and reduced cellular proliferation.

When the cohort of treated tumors was subdivided into responders versus nonresponders at a FDR of 1%, a list of 74 differentially expressed probes corresponding to 61 mouse genes was obtained (Supplementary Table S2B). These genes were more highly expressed in the mice that responded to treatment and the list was named RESP-HIGH. A GO analysis of the RESP-HIGH list revealed the presence of no significant GO terms after Bonferroni or Benjamini corrections. We also applied the 302 signatures analysis above on the responder versus nonresponder sample set, and only a small number of proliferation signatures was more highly expressed in nonresponders.

Human testing of the murine chemotherapy response signatures

Next, the murine 348 gene UNTREATED and 74 gene RESP-HIGH lists were converted into human lists using gene orthology, and both lists were then further refined using hierarchical cluster analyses of 337 human breast tumors from Prat and colleagues (ref. 1; Supplementary Fig. S2). This mouse-to-human filtering was necessary because a homogenous gene list from a cell line, or murine experiment, when applied to human primary tumors, will typically fragment into multiple signatures/modules when using *in vivo* human data (35). We observed this type of gene list heterogeneity here, and thus, from these cluster analyses, we chose a single dendrogram node that contained the

Published OnlineFirst June 18, 2013; DOI: 10.1158/1078-0432.CCR-13-0522

highest homogenously expressed gene set observed within this human primary tumor dataset, and for each gene list separately. This gave a set of 30 genes from the UNTREATED list that we call UNTREATED-HUM, and 12 genes from the RESP-HIGH list that we call RESP-HUM (Supplementary Fig. S2B and S2D); it should be noted that we did not test all possible dendrogram nodes, but instead limited our analyses to a single node from each cluster analysis. These 2 refined gene lists were also analyzed for GO terms with the UNTREATED-HUM list enriched for the terms "cell cycle," "M phase," "nuclear division," and "mitosis," and we also noted that 12 of the 30 entries were ATP-binding proteins. The RESP-HIGH was not enriched for any GO term.

We next tested both humanized gene lists for their ability to predict DRFS, and most importantly, pCR using a completely independent set of human patients with breast cancer treated with neoadjuvant chemotherapy. For both clinical endpoints, we used the Hatzis and colleagues dataset (see Fig. 1), which is a combined dataset of patients who were treated with a taxane and anthracycline-containing neoadjuvant chemotherapy regimen (28). We first stratified patients into low–medium–high (tertiles) groups based upon their rank-ordered mean expression values for the RESP-HUM and UNTREATED-HUM signature and then tested these stratifications for their ability to predict DRFS. These analyses showed that the RESP-HUM ($P < 0.001$) and UNTREATED-HUM ($P = 0.003$) signatures were able to predict DRFS, as was pCR versus not intrinsic subtype, and an 11-gene proliferation signature (Supplementary Fig. S3). In multivariable analyses (MVA), however, neither of these murine signatures added prognostic information beyond that conveyed by the PAM50 11-gene proliferation signature (ref. 9; data not shown).

We then tested the humanized gene lists for their ability to predict pCR, which is the most relevant endpoint for these chemotherapy response-based signatures. Within this patient set, 462 patients had pathologic response data; 91 patients achieved a pCR and 371 did not (20% overall pCR rate). The pCR rates varied according to intrinsic subtype as follows: Basal-like ($n = 129$, 40% pCR), Claudin-low ($n = 70$, 23% pCR), HER2-Enriched ($n = 27$, 19% pCR), Luminal A ($n = 140$, 3% pCR), Luminal B ($n = 68$, 16% pCR), and Normal-like ($n = 28$ total, 14% pCR). To determine the possible significance of our 2 response signatures on this test set of human patients, the mean expression values for each gene list were calculated and the distribution of values between pCR patients versus not pCR patients determined. As shown in Table 1, when all 473 patients were considered, the UNTREATED-HUM signature was significantly correlated with pCR ($P < 0.001$) and the RESP-HUM signature was trending toward significance ($P = 0.051$). As we further stratified patients into the 5 and even 6 intrinsic subtypes, the UNTREATED-HUM signature continued to maintain significance. Interestingly, the RESP-HUM signature predicted pCR more strongly in the Normal-like and Claudin-low subtypes, whereas the UNTREATED-HUM signature better tracked response within the Basal-like subtype

Table 1. pCR rates across different patient subsets for the RESP-HUM and UNTREATED-HUM signatures

			RESP-HUM			UNTREATED-HUM		
	pCR	Residual disease	*P*	AUC	OR	*P*	AUC	OR
All patients	91 (19.7%)	371 (80.3%)	0.051	0.586	0.788 (0.61–0.99)	<0.001	0.752	2.72 (2.08–3.63)
ER negative only	62 (33.3%)	124 (66.7%)	0.821			<0.001	0.683	2.09 (1.44–3.11)
ER positive only	29 (10.5%)	246 (89.5%)	0.405			<0.001	0.747	2.64 (1.67–4.31)
PAM50 (5 intrinsic subtypes)								
Basal-like	62 (35.8%)	111 (64.2%)	0.707			0.001	0.649	2.05 (1.33–3.24)
HER2-enriched	5 (17.9%)	23 (82.1%)	0.430			0.076		
Luminal A	4 (2.8%)	141 (97.2%)	0.208			0.172		
Luminal B	12 (16.7%)	60 (83.3%)	0.638			0.079		
Normal-like	8 (18.2%)	36 (81.8%)	0.009	0.837	4.47 (1.69–16.9)	0.274		
PAM50 + Claudin-low (6 intrinsic subtypes)								
Basal-like	51 (39.5%)	78 (60.5%)	0.356			0.001	0.680	2.33 (1.44–3.93)
Claudin-low	16 (22.9%)	54 (77.1%)	0.054	0.660	1.55 (1–2.47)	0.474		
HER2-enriched	5 (18.5%)	22 (81.5%)	0.426			0.086		
Luminal A	4 (2.9%)	136 (97.1%)	0.223			0.169		
Luminal B	11 (16.2%)	57 (83.8%)	0.976			0.272		
Normal-like	4 (14.3%)	24 (85.7%)	0.052			0.137		
Triple negative only	56 (33.5%)	111 (66.5%)	0.651			0.003	0.651	1.8 (1.24–2.68)

NOTE: The *P* value and AUC columns indicate whether the RESP-HUM or UNTREATED-HUM signature (as a continuous variable from low to high expression) was associated with response (italics) within that patient set/subset.

Published OnlineFirst June 18, 2013; DOI: 10.1158/1078-0432.CCR-13-0522

(Table 1). Finally, the TNBC distinction is a highly clinically relevant group because these patients are not candidates for the current targeted therapies in the breast clinic (10, 11); within this group, the UNTREATED-HUM signature was also a significant predictor ($P = 0.003$).

To more rigorously test the predictive significance of these new expression signatures, multivariable analysis using logistic regression was conducted that included the common clinical variables, the intrinsic subtypes, the RESP-HUM and UNTREATED-HUM signatures, and 3 predictive genomic signatures identified by Hatzis and colleagues (Table 2; ref. 28). For these analyses, we used the subset of patients that had pCR/response data, survival data, and who were treated with an anthracycline and taxane chemotherapy regimen ($n = 441$). As shown in Table 2, multiple biomarkers were predictive in univariate analyses, but only the UNTREATED-HUM, Basal-like, Normal-like, and one of the Hatzis and

Table 2. Univariate and MVA for pCR using clinical and genomic features including the RESP-HUM and UNTREATED-HUM signatures on the Hatzis and colleagues (28) dataset

		Univariate			Multivariate		
	No. of patients[a]	*P*	OR	AUC	*P*	OR	AUC
UNTREATED-HUM	441	<0.001	2.57 (1.96–3.45)	0.740	0.013	2.3 (1.21–4.52)	0.879
RESP-HUM	441	0.073	0.796 (0.618–1.02)	0.583	0.058	1.45 (0.99–2.15)	
PAM50 Proliferation	441	<0.001	2.57 (1.9–3.56)	0.730	0.917	0.96 (0.443–2.11)	
ER							
Negative	175 (40%)		1	0.562		1	
Positive	266 (60%)	<0.001	0.234 (0.139–0.385)		0.992	0.99 (0.391–2.52)	
PR							
Negative	227 (51%)		1	0.467			
Positive	214 (49%)	<0.001	0.30 (0.176–0.51)		0.683	0.83 (0.363–1.97)	
Clinical T stage							
1	27 (6%)		1	0.571		1	
2	226 (51%)	0.364	0.652 (0.269–1.75)		0.902	0.92 (0.261–3.39)	
3	126 (29%)	0.746	0.854 (0.34–2.36)		0.844	0.87 (0.236–3.38)	
4	62 (14%)	0.054	0.306 (0.0885–1.02)		0.195	0.35 (0.071–1.69)	
Clinical grade							
1	28 (6%)		1	0.481		1	
2	170 (39%)	0.498	2.05 (0.38–38.1)		0.967	1.05 (0.13–23.7)	
3	243 (55%)	0.019	11.1 (2.3–201)		0.574	2.02 (0.235–46.6)	
PAM50							
LumA	141 (32%)		1	0.633		1	
Basal	167 (38%)	<0.001	18.2 (7.21–61.5)		0.026	5.76 (1.3–29.4)	
Her2	24 (5%)	0.010	6.85 (1.51–31.1)		0.161	3.55 (0.59–21.7)	
LumB	67 (15%)	0.003	6.01 (1.92–22.6)		0.400	1.92 (0.438–9.49)	
Normal	42 (10%)	0.001	8.06 (2.39–31.7)		0.002	10 (2.34–47.6)	
Hatzis signature SET index							
1	386 (88%)		1	0.136		1	
2	36 (8%)	0.091	0.353 (0.0835–1.02)		0.729	1.34 (0.223–6.49)	
3	19 (4%)	0.302	0.457 (0.0715–1.64)		0.953	0.94 (0.105–6.17)	
Hatzis signature chemosensitive (RCB-I predict)							
1	296 (67%)		1	0.553		1	
2	145 (33%)	<0.001	2.97 (1.82–4.84)		0.127	1.76 (0.855–3.67)	
Hatzis signature chemoresistance (RCB-III predict or 3-year survival)							
1	197 (45%)		1	0.603		1	
2	244 (55%)	<0.001	0.089 (0.0449–0.166)		<0.001	0.129 (0.0565–0.277)	

NOTE: Univariate and MVAs were conducted using all Hatzis and colleagues (28) patients who received anthracycline and taxane chemotherapy only, and who had overall survival data ($n = 441$).

[a]The number of patients with clinical ER status, PR status, T stage, grade, and pCR status available.

Published OnlineFirst June 18, 2013; DOI: 10.1158/1078-0432.CCR-13-0522

colleagues chemotherapy predictor signatures (i.e., RCB-III/resistance) were found significant in both the univariate and multivariate tests (28). To further assess the strength of the predictive powers of these genomic signatures, each was used to calculate an AUC for pCR, both alone (univariate AUC) and in the multivariate model (Table 2). The UNTREAT-HUM signature provided a good univariate AUC, and the multivariate model provided improvement with a high AUC (0.879). When the 3 Hatzis and colleagues signatures were removed from the MVA, most of the variables that were significant in the initial MVA remained significant, and the overall model continued to show a high AUC (0.82; data not shown; ref. 28). Finally, an additional test dataset of anthracycline and taxane-treated human patients was tested, which represents 81 patients treated neoadjuvantly from Japan (29); similar predictive results were seen for the UNTREAT-HUM signature, which was again a significant predictor in both the univariate and MVAs (Supplementary Table S4). These data show that the UNTREATED-HUM signature (and possibly the RESP-HUM) provided predictive information for pCR beyond (i) the commonly used clinical variables, (ii) breast cancer subtype, and (iii) other genomic signatures derived from one of the datasets tested here.

Discussion

As new agents for breast cancers are developed, validated preclinical models for assessing these agents' activity alone and in combination with approved therapies are needed. In this study, we chose genomically credentialed GEMM representatives for 3 human breast tumor subtypes (Basal-like, Luminal B, and Claudin-low) as our preclinical models. Although using single representatives of different tumor subtypes does not allow for the identification of subtype-specific effects, we believe that this approach does make future predictions of therapeutic efficacy more robust by including results from a biologically diverse group of tumor-bearing individuals.

For therapeutic efficacy, each GEMM was treated with identical regimens and for most drugs, variable responses were seen. Our findings show that the *MMTV-Neu* tumors were the most responsive in general, with multiple agents being able to achieve complete tumor regression, especially the HER2-targeted agent lapatinib. Next in sensitivities was the Basal-like *C3(1)-T-antigen* model, which was generally more resistant than the *MMTV-Neu* model, but in some cases complete responses were documented (CT and carboplatin/erlotinib); interestingly, a heterogeneity of responses was common in this GEMM (Fig. 2A), suggesting that 2 or more subclasses of tumors may be present. Importantly, a similar heterogeneous response pattern is seen within human patients with Basal-like when treated with comparable agents where many patients achieve a pCR and have good overall survival, but the majority show residual disease and worse outcomes (Supplementary Fig. S3C and see refs. 5, 36). Finally, the Claudin-low *T11/TP53*$^{-/-}$ model was the most resistant with only small responses seen in this model.

We ultimately chose to focus our analysis on expression signatures associated with chemotherapy treatment of one of our GEMMs and response for 2 main reasons. First, we reasoned that transcripts highly expressed in sensitive murine tumors (i.e., the RESP-HIGH list) might also be highly expressed in sensitive human tumors; although this list was predictive in human tumors, it was not obvious from GO analysis what molecular characteristics drive this biology, and this list was not significant when accounting for other variables (MVA $P = 0.058$). Second, in a tumor treated *in vivo*, we reasoned chemotherapy might deplete the most sensitive cells and their characteristic transcripts. Therefore, the collection of transcripts that were highly expressed in untreated cells and depleted with treatment (i.e., the UNTREATED list) similarly seemed rational for testing in humans. Specifically, an analysis showed that the 26-gene UNTREAT-HUM signature (Supplementary Fig. S3) was a significant predictor of response and may also provide mechanistic insight. This 26-gene list suggests that the cells actually undergoing DNA synthesis and mitosis (i.e., in S–G_2–M phase) are more sensitive to cytotoxic agents than cells in other parts of the cell cycle (G_0 or G_1), which is a concept dating back to the 1960s (reviewed in ref. 37). It is important to note that this list added independent information above and beyond strict assessments of proliferation (e.g., an 11-gene proliferation signature that contains Ki-67), suggesting this list may better capture specific features of the cell cycle (e.g., length of time spent in S–G_2–M) associated with sensitivity to carboplatin/paclitaxel. The UNTREAT-HUM list is in fact a biologically rich list that contains at least 2 different sets of genes/proteins that physically form a multiprotein complex, namely SMC2 and SMC4, and MCM4 and MCM6. In addition, this list has 2 different E2F family members (E2F3 and E2F8), for which a poor prognostic signature has already been linked to E2F3 (38). These data also suggest that no single gene/protein is likely to be a robust biomarker of chemosensitivity because a multitude of genes, each involved in different aspects of the cell cycle, were collectively identified as being predictive of response. These new expression signatures were derived from murine models that, despite their specific chemoresponses not being a mirror of their human counterparts (i.e., paclitaxel), added a significant predictive component to the multivariate model that at least equaled the ability of those tested signatures that were derived directly from this human tumor dataset.

In terms of human biomarker advances, we made progress using the *C3(1)-Tag* GEMM. As shown in Tables 1 and 2, the UNTREATED-HUM signature was predictive of response to a multi-agent neoadjuvant chemotherapy regimen, not only across all human patients with HER2-normal breast cancer but also within the clinically relevant triple-negative subset, as well as the more biologically relevant Basal-like subset. Interestingly, this UNTREATED-HUM signature was also able to predict pCR even when accounting for intrinsic subtype, the common clinical variables, and 2 other genomic signatures specifically designed to predict neoadjuvant response (Table 2). Although the

Published OnlineFirst June 18, 2013; DOI: 10.1158/1078-0432.CCR-13-0522

murine treatment and human treatment involved the use of different chemotherapeutics, both species studies used paclitaxel and at least one DNA-damaging agent (carboplatin in mice and doxorubicin/epirubicin in humans). Overall, a multivariate model that contained the UNTREAT-HUM, the intrinsic subtypes, and the common clinical variables showed an AUC of 0.82, which may be sufficiently predictive to be of value for routine clinical use.

We were surprised to find that the results from mice treated with single-agent paclitaxel did not mimic the effectiveness of this drug in human patients with breast cancer. Delivery of higher therapeutic doses of paclitaxel to the mice (i.e., doses closer to those received by human patients) may have proven more efficacious; however, our chosen formulation of paclitaxel contained chremaphor and ethanol in amounts that precluded higher dosing. Another caveat to our studies is that these 2 GEMM-derived signatures were both predictive and prognostic; however, it must be noted that it is often difficult, if not impossible, to disentangle these 2 features. For example, both ER and HER2 in breast cancer are prognostic (they predict outcomes in the absence of therapy) and they are predictive (ER predicts hormone therapy benefit and HER2 predicts trastuzumab benefit) and thus, our new signatures are showing dual properties similar to those seen for the existing breast cancer biomarkers. Much additional validation work is needed before these 2 murine-derived signatures could be used to guide patient treatment. However, this study has laid the groundwork of a general strategy for evaluating new drugs, combinations, and schedules using GEMMs and has shown that it is possible to use mice as a tool to identify a biomarker that may be of predictive value for human patients with cancer.

Disclosure of Potential Conflicts of Interest

C.M. Perou is employed (other than primary affiliation; e.g., consulting) as a board member and has ownership interest (including patents) in University Genomics and Bioclassifier LLC. No potential conflicts of interest were disclosed by the other authors.

Authors' Contributions

Conception and design: J.E. Usary, N. Sharpless, C.M. Perou
Development of methodology: J.E. Usary, O. Karginova, A. Combest, A. Prat, C.M. Perou
Acquisition of data (provided animals, acquired and managed patients, provided facilities, etc.): J.E. Usary, D. Darr, P.J. Roberts, M. Liu, O. Karginova, A. Combest, A.S. Bridges, A. Prat, M.C.U. Cheang, J.I. Herschkowitz, J.M. Rosen
Analysis and interpretation of data (e.g., statistical analysis, biostatistics, computational analysis): J.E. Usary, W. Zhao, P.J. Roberts, J. Jordan, A. Combest, A. Prat, M.C.U. Cheang, N. Sharpless, C.M. Perou
Writing, review, and/or revision of the manuscript: J.E. Usary, W. Zhao, P.J. Roberts, A. Combest, A. Prat, J.I. Herschkowitz, N. Sharpless, C.M. Perou
Administrative, technical, or material support (i.e., reporting or organizing data, constructing databases): J.E. Usary, D. Darr, L. Balletta, O. Karginova, M.C.U. Cheang
Study supervision: J.E. Usary, W. Zamboni, C.M. Perou

Grant Support

This work was supported by funding from the National Cancer Institute Breast SPORE program (P50-CA58223-09A1), by RO1-CA138255 and RO1-CA148761, by the Breast Cancer Research Foundation, and by a generous gift to the UNC Mouse Phase I Unit.

The costs of publication of this article were defrayed in part by the payment of page charges. This article must therefore be hereby marked *advertisement* in accordance with 18 U.S.C. Section 1734 solely to indicate this fact.

Received February 25, 2013; revised June 4, 2013; accepted June 9, 2013; published OnlineFirst June 18, 2013.

References

1. Prat A, Parker JS, Karginova O, Fan C, Livasy C, Herschkowitz JI, et al. Phenotypic and molecular characterization of the claudin-low intrinsic subtype of breast cancer. Breast Cancer Res 2010;12:R68.
2. Parker JS, Mullins M, Cheang MC, Leung S, Voduc D, Vickery T, et al. Supervised risk predictor of breast cancer based on intrinsic subtypes. J Clin Oncol 2009;27:1160–7.
3. Hu Z, Fan C, Oh DS, Marron JS, He X, Qaqish BF, et al. The molecular portraits of breast tumors are conserved across microarray platforms. BMC Genomics 2006;7:96.
4. Hugh J, Hanson J, Cheang MC, Nielsen TO, Perou CM, Dumontet C, et al. Breast cancer subtypes and response to docetaxel in node-positive breast cancer: use of an immunohistochemical definition in the BCIRG 001 trial. J Clin Oncol 2009;27:1168–76.
5. Carey LA, Dees EC, Sawyer L, Gatti L, Moore DT, Collichio F, et al. The triple negative paradox: primary tumor chemosensitivity of breast cancer subtypes. Clin Cancer Res 2007;13:2329–34.
6. Martin M, Romero A, Cheang MC, López García-Asenjo JA, García-Saenz JA, Oliva B, et al. Genomic predictors of response to doxorubicin versus docetaxel in primary breast cancer. Breast Cancer Res Treat 2011;128:127–36.
7. Gluck S, Ross JS, Royce M, McKenna EF Jr, Perou CM, Avisar E, et al. TP53 genomics predict higher clinical and pathologic tumor response in operable early-stage breast cancer treated with docetaxel-capecitabine ± trastuzumab. Breast Cancer Res Treat 2012; 132:781–91.
8. Dunbier AK, Anderson H, Ghazoui Z, Salter J, Parker JS, Perou CM, et al. Association between breast cancer subtypes and response to neoadjuvant anastrozole. Steroids 2011;76:736–40.
9. Nielsen TO, Parker JS, Leung S, Voduc D, Ebbert M, Vickery T, et al. A comparison of PAM50 intrinsic subtyping with immunohistochemistry and clinical prognostic factors in tamoxifen-treated estrogen receptor-positive breast cancer. Clin Cancer Res 2010;16:5222–32.
10. Perou CM. Molecular stratification of triple-negative breast cancers. Oncologist 2011;16 Suppl 1:61–70.
11. Prat A, Adamo B, Cheang MC, Anders CK, Carey LA, Perou CM. Molecular characterization of basal-like and non-basal-like triple-negative breast cancers. Oncologist 2013;18:123–33.
12. Herschkowitz JI, Zhao W, Zhang M, Usary J, Murrow G, Edwards D, et al. Breast cancer special feature: comparative oncogenomics identifies breast tumors enriched in functional tumor-initiating cells. Proc Natl Acad Sci U S A 2012;109:2778–83.
13. Van Dyke T, Jacks T. Cancer modeling in the modern era: progress and challenges. Cell 2002;108:135–44.
14. Sharpless NE, Depinho RA. The mighty mouse: genetically engineered mouse models in cancer drug development. Nat Rev Drug Discov 2006;5:741–54.
15. Roberts PJ, Usary JE, Darr DB, Dillon PM, Pfefferle AD, Whittle MC, et al. Combined PI3K/mTOR and MEK inhibition provides broad anti-tumor activity in faithful murine cancer models. Clin Cancer Res 2012; 18:5290–303.
16. Chen Z, Cheng K, Walton Z, Wang Y, Ebi H, Shimamura T, et al. A murine lung cancer co-clinical trial identifies genetic modifiers of therapeutic response. Nature 2012;483:613–7.
17. Nardella C, Lunardi A, Patnaik A, Cantley LC, Pandolfi PP. The APL paradigm and the "co-clinical trial" project. Cancer Discov 2011;1: 108–16.

Published OnlineFirst June 18, 2013; DOI: 10.1158/1078-0432.CCR-13-0522

18. Herschkowitz JI, Simin K, Weigman VJ, Mikaelian I, Usary J, Hu Z, et al. Identification of conserved gene expression features between murine mammary carcinoma models and human breast tumors. Genome Biol 2007;8:R76.
19. Maroulakou IG, Anver M, Garrett L, Green JE. Prostate and mammary adenocarcinoma in transgenic mice carrying a rat C3(1) simian virus 40 large tumor antigen fusion gene. Proc Natl Acad Sci U S A 1994;91: 11236–40.
20. Guy CT, Webster MA, Schaller M, Parsons TJ, Cardiff RD, Muller WJ. Expression of the neu protooncogene in the mammary epithelium of transgenic mice induces metastatic disease. Proc Natl Acad Sci U S A 1992;89:10578–82.
21. Green JE, Shibata MA, Yoshidome K, Liu ML, Jorcyk C, Anver MR, et al. The C3(1)/SV40 T-antigen transgenic mouse model of mammary cancer: ductal epithelial cell targeting with multistage progression to carcinoma. Oncogene 2000;19:1020–7.
22. Jerry DJ, Kittrell FS, Kuperwasser C, Laucirica R, Dickinson ES, Bonilla PJ, et al. A mammary-specific model demonstrates the role of the p53 tumor suppressor gene in tumor development. Oncogene 2000;19: 1052–8.
23. Hou W, Watters JW, McLeod HL. Simple and rapid docetaxel assay in plasma by protein precipitation and high-performance liquid chromatography-tandem mass spectrometry. J Chromatogr B Analyt Technol Biomed Life Sci 2004;804:263–7.
24. Eisen MB, Spellman PT, Brown PO, Botstein D. Cluster analysis and display of genome-wide expression patterns. Proc Natl Acad Sci U S A 1998;95:14863–8.
25. Saldanha AJ. Java Treeview–extensible visualization of microarray data. Bioinformatics 2004;20:3246–8.
26. Tusher VG, Tibshirani R, Chu G. Significance analysis of microarrays applied to the ionizing radiation response. Proc Natl Acad Sci U S A 2001;98:5116–21.
27. Spector NL, Xia W, Burris H III, Hurwitz H, Dees EC, Dowlati A, et al. Study of the biologic effects of lapatinib, a reversible inhibitor of ErbB1 and ErbB2 tyrosine kinases, on tumor growth and survival pathways in patients with advanced malignancies. J Clin Oncol 2005;23:2502–12.
28. Hatzis C, Pusztai L, Valero V, Booser DJ, Esserman L, Lluch A, et al. A genomic predictor of response and survival following taxane-anthracycline chemotherapy for invasive breast cancer. JAMA 2011;305: 1873–81.
29. Miyake T, Nakayama T, Naoi Y, Yamamoto N, Otani Y, Kim SJ, et al. GSTP1 expression predicts poor pathological complete response to neoadjuvant chemotherapy in ER-negative breast cancer. Cancer Sci 2012;103:913–20.
30. Harris L, Fritsche H, Mennel R, Norton L, Ravdin P, Taube S, et al. American Society of Clinical Oncology 2007 update of recommendations for the use of tumor markers in breast cancer. J Clin Oncol 2007;25:5287–312.
31. Tutt AN, Lord CJ, McCabe N, Farmer H, Turner N, Martin NM, et al. Exploiting the DNA repair defect in BRCA mutant cells in the design of new therapeutic strategies for cancer. Cold Spring Harb Symp Quant Biol 2005;70:139–48.
32. Hidalgo M, Siu LL, Nemunaitis J, Rizzo J, Hammond LA, Takimoto C, et al. Phase I and pharmacologic study of OSI-774, an epidermal growth factor receptor tyrosine kinase inhibitor, in patients with advanced solid malignancies. J Clin Oncol 2001;19:3267–79.
33. Fan C, Prat A, Parker JS, Liu Y, Carey LA, Troester MA, et al. Building prognostic models for breast cancer patients using clinical variables and hundreds of gene expression signatures. BMC Med Genomics 2011;4:3.
34. Creighton CJ, Li X, Landis M, Dixon JM, Neumeister VM, Sjolund A, et al. Residual breast cancers after conventional therapy display mesenchymal as well as tumor-initiating features. Proc Natl Acad Sci U S A 2009;106:13820–5.
35. Hoadley KA, Weigman VJ, Fan C, Sawyer LR, He X, Troester MA, et al. EGFR associated expression profiles vary with breast tumor subtype. BMC Genomics 2007;8:258.
36. Liedtke C, Mazouni C, Hess KR, André F, Tordai A, Mejia JA, et al. Response to neoadjuvant therapy and long-term survival in patients with triple-negative breast cancer. J Clin Oncol 2008;26: 1275–81.
37. Norton L. Implications of kinetic heterogeneity in clinical oncology. Semin Oncol 1985;12:231–49.
38. Huang E, Ishida S, Pittman J, Dressman H, Bild A, Kloos M, et al. Gene expression phenotypic models that predict the activity of oncogenic pathways. Nat Genet 2003;34:226–30.